JOURNAL OF GUIDANCE, CONTROL, AND DYNAMICS
Vol. 20, No. 5, September–October 1997

Adaptive Nonlinear Attitude Control and Momentum Management of Spacecraft

Scott J. Paynter* and Robert H. Bishop†
University of Texas at Austin, Austin, Texas 78712

An indirect adaptive nonlinear controller is investigated for attitude control and momentum management of evolutionary spacecraft. The control law is based on the theory of nonlinear feedback linearization. A new state transformation is introduced: one that converts the original nonlinear system into normal canonical form. Once in canonical form, nonlinear feedback is used to generate a linear response in the transformed coordinates. To make the nonlinear controller adaptive, a parameter identification scheme, utilizing an extended Kalman filter, is added for mass property estimation. Probing signals are introduced to enhance the observability of the mass properties. Simulation results show that the adaptive nonlinear controller stabilizes the International Space Station during mass property changes, successfully performs momentum management, and provides real-time estimates of the mass properties in a realistic environment.

Introduction

WITH the development of the space station, there has been a shift in design methodology from single-task spacecraft to multipurpose spacecraft, which can evolve to perform multiple missions. The multipurpose spacecraft operates in many different configurations as the vehicle evolves. With the increased use of spacecraft that operate under a wide variety of conditions and changing configurations, the need for controllers that can adjust to these changes becomes essential for proper attitude stabilization. This paper proposes an indirect adaptive controller to stabilize these evolutionary spacecraft. The proposed scheme is based on the idea of feedback linearization of the attitude dynamics and control moment gyro (CMG) dynamics, and the utilization of an extended Kalman filter (EKF) for parameter estimation.

The main problem can be stated as follows: develop an attitude control scheme that stabilizes a spacecraft during configuration changes and properly manages the stored CMG momentum. This will be referred to as the attitude control and momentum management (ACMM) problem. This problem is important because during the life span of an evolutionary spacecraft numerous configuration changes can occur that may affect the stability of the onboard attitude control law. Because each configuration may require its own controller design, a multitude of possible controllers may need to be designed and implemented during an evolutionary spacecraft's operational lifetime. If a control law can be developed that automatically adjusts to the configuration changes, then only one controller needs to be designed and implemented onboard the spacecraft.

During the life span of a spacecraft, certain attitude orientations are expected so that normal interface with ground bases and other spacecraft can be maintained. To accomplish this, the spacecraft needs an attitude control system (ACS) capable of applying control torques to guarantee proper spacecraft pointing. Spacecraft may use CMGs as their principal actuators. However, CMGs are momentum exchangers, which can only store a certain amount of momentum, and so desaturation by external torques is necessary. Several methods for desaturating the CMGs are available, but gravity gradient torques are preferred because no additional actuating systems, such as reaction control jets, are required.

During many operating conditions, spacecraft may be expected to maintain local vertical/local horizontal (LVLH) attitude. Unfortunately, for most configurations, maintaining LVLH attitude requires the CMGs to continuously exchange momentum. This is clearly not possible without other external torques desaturating the CMGs. Therefore, an ACS is needed that can maintain the desired orientation of the spacecraft, as well as perform momentum management for the CMGs. Using gravity gradient torques as CMG desaturators can lead to torque equilibrium attitudes (TEAs) that do not correspond to LVLH attitude. Thus, combining ACMM becomes a problem of compromise. A balance between correct spacecraft pointing and stored CMG momentum is required. This is the job of the attitude control and momentum manager.

The space station project has motivated numerous recent investigations into the problem of ACMM of spacecraft using CMGs.[1–20] Many ACMM systems have been developed based on linearized dynamic models.[1–11] In the conventional linear system design approach, a linear approximation of the system dynamics is obtained by using Taylor series expansions and neglecting higher-order terms. Usually, when classical linearization is employed in the ACMM problem, an LVLH attitude history is taken as the reference trajectory and the cross products of inertia are neglected. A linear (fixed-gain) controller is generally developed from these linear models.

Inasmuch as evolutionary spacecraft can undergo substantial mass property and configuration changes, one approach to the problem is to employ robust linear control design methods. Researchers have investigated controllers based on linear quadratic regulator, H_∞, and other robust methodologies.[3–7]

Nonlinear methods have been shown to be directly applicable to the ACMM problem.[12–20] Vadali and Oh[12] used Lyapunov's second method to develop a nonlinear ACMM control law that guarantees closed-loop stability. Several nonlinear controllers for ACMM have been developed based on feedback linearization.[13–17] The main idea behind this nonlinear control approach is to transform the nonlinear system into a normal canonical form (valid in a region about the TEA) and then exactly cancel the nonlinear dynamics. This process leads to a system that behaves linearly in the neighborhood of the TEA. Singh and Bossart[13,14] and Singh and Iyer[15] assume small roll and yaw angles and neglect the cross products of inertia, thus neglecting some of the nonlinear dynamics. Sheen and Bishop[16] do not make small angle assumptions, but do require zero cross products of inertia. Their control law allows for large vehicle angles and rates and large CMG momentum. Dzielski et al.[17] account for the cross products of inertia, but the control law is never expressed explicitly.

This paper describes an adaptive nonlinear approach to the ACMM problem in the presence of mass property uncertainty. An

Presented as Paper 95-418 at the AAS/AIAA Astrodynamics Conference, Halifax, NS, Canada, Aug. 14–17, 1995; received July 18, 1996; revision received April 25, 1997; accepted for publication May 12, 1997.

*Graduate Student, Department of Aerospace Engineering and Engineering Mechanics. E-mail: paynter@vs.lmco.com. Member AIAA.

†Associate Professor, Department of Aerospace Engineering and Engineering Mechanics. Senior Member AIAA.

adaptive nonlinear controller addresses the mass property uncertainty and eliminates the need for making assumptions of small angles and rates, small CMG momentum, and negligible cross products of inertia.

Adaptive controllers are capable of learning about their environments and then adapting to them.[21] When adaptive controllers use the knowledge learned about their surroundings, they can alter themselves internally to maintain a given set of performance specifications. Both direct and indirect methods of adaptive control are available for the ACMM problem. Direct adaptive controllers generally utilize a tracking-error-based algorithm, where changes in the control law are made based on the differences between where the system is and where the adaptive controller thinks the system should be. In general, stability guarantees can be obtained using Lyapunov stability analysis for direct adaptive controllers. A direct adaptive control scheme using feedback linearization was developed by Sheen and Bishop[18] for spacecraft with uncertain mass properties. Burns and Flashner[8] designed a model reference adaptive controller for unloading angular momentum from spacecraft in a low Earth orbit, but used linearized dynamical equations.

Indirect adaptive controllers use parameter identification schemes to explicitly estimate parameters in the dynamic system. Measurements of the time-varying system (such as Euler angles and body rates) are utilized by a parameter identification scheme to determine the changing system parameters (such as the inertia matrix). The parameter estimates are processed by a controller redesign algorithm to meet the given performance specifications. The new controller parameters are then provided to the control algorithm, which continues stabilizing the closed-loop system.

Zhao et al.[9] have proposed one type of indirect adaptive scheme for adaptive control of the space station: a hybrid state-space self-tuning controller that estimates discrete-time parameters of the continuous-time system and uses these estimates in an optimal pole-placement algorithm. This controller is based on a linearized model of the dynamics. Another self-tuning approach has been developed by Paynter[19] for the attitude control problem (without momentum management) with a full inertia matrix and without linearization of the system dynamics. In this paper, the work in Ref. 19 is expanded to include the momentum management aspect.

Other adaptive control methodologies, such as gain scheduling, are also possible. However, gain scheduling still requires designing a family of controllers that can account for all possible spacecraft configurations. Depending on the range of mass property variations, the number of individual controllers required can become quite large, and a method for switching between the controllers would be necessary. A gain scheduled approach was taken by Parlos and Sunkel.[10]

Mathematical Models

In the proposed control system design, a nonlinear model for the spacecraft's attitude is used. The model includes the attitude kinematics, the rotational dynamics, and the CMG momentum dynamics. These equations have appeared in the literature previously.[1,16,17] An Earth-pointing spacecraft in a circular low Earth orbit is considered.

The relevant coordinate systems are the LVLH frame (denoted by L), the body frame (denoted by B), and the principal body frame (denoted by P), each of which originates at the center of mass of the spacecraft. The Z_L axis originates at the center of mass of the spacecraft and passes through the center of the Earth, which is assumed inertially fixed. The X_L–Z_L plane corresponds to the instantaneous orbit plane. The Y_L axis points in the opposite direction of the instantaneous orbital angular momentum vector. The direction of the X_L axis is chosen to complete the right-handed coordinate system and points in the direction of the spacecraft velocity. The LVLH frame rotates about the $-Y_L$ axis at the orbital rate η of the spacecraft. The body axes are fixed to the spacecraft and are orthogonal.

The orientation of the body frame relative to the LVLH frame is described by a sequence of three rotations: pitch–yaw–roll. The transformation $\boldsymbol{T}^{BL}$, which takes vectors $\boldsymbol{v}^L$ in the LVLH frame to vectors $\boldsymbol{v}^B$ in the body frame, is given such that

$$\boldsymbol{v}^B = \boldsymbol{T}^{BL}\boldsymbol{v}^L \tag{1}$$

where

$$\boldsymbol{T}^{BL} = \begin{bmatrix} c_p c_y & s_y & -s_p c_y \\ s_r s_p - c_r c_p s_y & c_r c_y & s_r c_p + c_r s_p s_y \\ c_r s_p + s_r c_p s_y & -s_r c_y & c_r c_p - s_r s_p s_y \end{bmatrix} \tag{2}$$

with $c_i = \cos\theta_i$ and $s_i = \sin\theta_i$ for $i = r, p, y$, where θ_r is the roll angle, θ_p is the pitch angle, and θ_y is the yaw angle. Inasmuch as $\boldsymbol{T}^{BL}$ is orthonormal, $\boldsymbol{T}^{LB} = (\boldsymbol{T}^{BL})^T$, where the superscript T indicates the matrix transpose.

Because we are considering a spacecraft with time-varying mass properties, the principal body frame can change its orientation relative to the spacecraft. Therefore, it is not convenient to present the dynamical equations relative to the P frame. However, in some of the analysis it is convenient to present the results in terms of the principal inertias and the principal Euler angles (denoted by $\boldsymbol{\theta}^*$). The principal Euler angles represent the orientation of the principal axes relative to the LVLH frame.

For a pitch–yaw–roll rotation sequence, the attitude kinematics for a spacecraft in a circular orbit are given by

$$\dot{\boldsymbol{\theta}} = \boldsymbol{R}\boldsymbol{\omega}_B^B + \boldsymbol{\eta} \tag{3}$$

where

$$\boldsymbol{R} = \begin{bmatrix} 1 & -\cos\theta_r \tan\theta_y & \sin\theta_r \tan\theta_y \\ 0 & \dfrac{\cos\theta_r}{\cos\theta_y} & -\dfrac{\sin\theta_r}{\cos\theta_y} \\ 0 & \sin\theta_r & \cos\theta_r \end{bmatrix} \tag{4}$$

and $\boldsymbol{\theta} = (\theta_r, \theta_p, \theta_y)^T$, $\boldsymbol{\omega}_B^B$ is the spacecraft angular rate, $\boldsymbol{\eta} = (0, \eta, 0)^T$, and $\boldsymbol{\eta}$ is the spacecraft orbital rate.

For design purposes, the spacecraft is considered to be a rigid body. The rotational dynamics of a rigid spacecraft are given by Euler's equation

$$\boldsymbol{I}_B^B\dot{\boldsymbol{\omega}}_B^B = -\boldsymbol{\omega}_B^B \times \boldsymbol{I}_B^B\boldsymbol{\omega}_B^B + \boldsymbol{\tau}_{\text{gg}}^B - \boldsymbol{u}^B + \boldsymbol{\tau}_{\text{dist}}^B \tag{5}$$

where $\boldsymbol{I}_B^B$ is the spacecraft inertia matrix relative to the body frame, $\boldsymbol{u}^B$ is the interactive CMG control torque, $\boldsymbol{\tau}_{\text{gg}}^B$ is the gravity gradient torque, and $\boldsymbol{\tau}_{\text{dist}}^B$ is any other disturbance torque acting on the spacecraft, such as aerodynamic torques. For a spacecraft in a circular orbit, the gravity gradient torque $\boldsymbol{\tau}_{\text{gg}}$ is given by

$$\boldsymbol{\tau}_{\text{gg}} = 3\eta^2\boldsymbol{k}_L \times \boldsymbol{I}_B\boldsymbol{k}_L \tag{6}$$

where $\boldsymbol{k}_L$ is the unit vector in the direction of the Z_L axis. The disturbance torque $\boldsymbol{\tau}_{\text{dist}}^B$ is assumed small and is neglected in the nonlinear controller design (but not in the simulations).

The dynamics of the CMG momentum, $\boldsymbol{h}_W^B$, are given by

$$\dot{\boldsymbol{h}}_W^B = -\boldsymbol{\omega}_B^B \times \boldsymbol{h}_W^B + \boldsymbol{u}^B \tag{7}$$

For this analysis, the CMGs are assumed to be ideal momentum exchange devices, i.e., the internal dynamics of the CMGs are neglected and the momentum is exchanged directly through the interactive control torque $\boldsymbol{u}$.

The equations of motion can also be written in the LVLH frame. To do so, we must first compute the time derivatives of $\boldsymbol{T}^{BL}$ and $\boldsymbol{I}_B^L$, the inertia of the spacecraft relative to the LVLH frame. The transformation matrix $\boldsymbol{T}^{LB}$ is a function of time and has a time derivative given by

$$\dot{\boldsymbol{T}}^{LB} = \boldsymbol{\Omega}_{B\,|\,L}^L\boldsymbol{T}^{LB} \tag{8}$$

where $\boldsymbol{\Omega}_{B\,|\,L}^L$ is the skew-symmetric matrix

$$\boldsymbol{\Omega}_{B\,|\,L}^L = \begin{bmatrix} 0 & -\omega_{B_3}^L & \omega_{B_2}^L + \eta \\ \omega_{B_3}^L & 0 & -\omega_{B_1}^L \\ -\omega_{B_2}^L - \eta & \omega_{B_1}^L & 0 \end{bmatrix} \tag{9}$$

In the LVLH frame, the inertia matrix varies with time. The inertia matrix in the LVLH axes is related to the inertia matrix in the body axes through the similarity transformation

$$\boldsymbol{I}_B^L = \boldsymbol{T}^{LB}\boldsymbol{I}_B^B\boldsymbol{T}^{BL} \tag{10}$$

Taking the time derivative of $\boldsymbol{I}^L$ and simplifying yields

$$\dot{\boldsymbol{I}}_B^L = \boldsymbol{\Omega}_{B\,|\,L}^L\boldsymbol{I}_B^L - \boldsymbol{I}_B^L\boldsymbol{\Omega}_{B\,|\,L}^L \tag{11}$$

Because each $\dot{I}_{B_{ij}}^L$ includes terms containing $\boldsymbol{\omega}_B^L$, differentiating $\dot{\boldsymbol{I}}_B^L$ further will lead to explicit terms containing elements of $\boldsymbol{u}$. This fact is used shortly.

The angular rate of the spacecraft relative to the L frame is related to $\boldsymbol{\omega}_B^B$ by

$$\boldsymbol{\omega}_B^L = \boldsymbol{T}^{LB}\boldsymbol{\omega}_B^B \tag{12}$$

Taking the time derivative of $\boldsymbol{\omega}_B^L$ and further simplifying yields

$$\dot{\boldsymbol{\omega}}_B^L = \left(\boldsymbol{I}_B^L\right)^{-1}\left(-\boldsymbol{\omega}_B^L \times \boldsymbol{I}_B^L\boldsymbol{\omega}_B^L + 3\eta^2\boldsymbol{k}_L^L \times \boldsymbol{I}_B^L\boldsymbol{k}_L^L - \boldsymbol{u}^L\right) + \boldsymbol{\eta} \times \boldsymbol{\omega}_B^L \tag{13}$$

where $\boldsymbol{I}_B^L$ varies with time according to Eq. (11).

The total angular momentum of the spacecraft system, $\boldsymbol{h}_B$, is given by

$$\boldsymbol{h}_B = \boldsymbol{h}_W + \boldsymbol{I}_B\boldsymbol{\omega}_B \tag{14}$$

Taking the first and second time derivatives of $\boldsymbol{h}_B$ relative to the L frame and simplifying yields

$$\dot{\boldsymbol{h}}_B^L = \begin{pmatrix} \eta h_{B_3}^L - 3\eta^2 I_{B_{23}}^L \\ 3\eta^2 I_{B_{13}}^L \\ -\eta h_{B_1}^L \end{pmatrix} \tag{15}$$

and

$$\ddot{\boldsymbol{h}}_B^L = \begin{pmatrix} -\eta^2 h_{B_1}^L - 3\eta^2 \dot{I}_{B_{23}}^L \\ 3\eta^2 \dot{I}_{B_{13}}^L \\ -\eta^2 h_{B_3}^L + 3n^3 I_{B_{23}}^L \end{pmatrix} \tag{16}$$

Note that, because $\dot{h}_{B_3}^L = -\eta h_{B_1}^L$, the third derivative of $h_{B_3}^L$ is

$$\dddot{h}_{B_3}^L = -\eta\ddot{h}_{B_1}^L = \eta^3 h_{B_1}^L + 3\eta^3 \dot{I}_{B_{23}}^L \tag{17}$$

As mentioned, taking a second derivative of any of the $\boldsymbol{I}_B^L$ terms will lead to terms containing elements of the control vector $\boldsymbol{u}$. Thus, $h_{B_1}^L$ and $h_{B_2}^L$ can be differentiated three times before any element of $\boldsymbol{u}$ will appear, whereas $h_{B_3}^L$ can be differentiated four times before any control appears. Therefore, $h_{B_1}^L$ and $h_{B_2}^L$ have relative degree three, whereas $h_{B_3}^L$ has relative degree four. (See Ref. 22 for more on relative degree.)

Nonlinear Controller Design

In this section, a feedback control law that exactly linearizes the spacecraft dynamics system is developed, without relying on any standard linearization approximations (such as small angles, rates, and negligible cross products of inertia). In this linearizing process, a state transformation that transforms the nonlinear system into normal canonical form is introduced. Then, in the transformed state, a linearizing feedback control law is developed. For an in-depth discussion of the theory behind feedback linearization and its solution, the reader is directed to Ref. 22 or 23. Several investigations have verified that the necessary conditions for using feedback linearization have been met for both the attitude control and the ACMM problems.[16,17,20]

Note that not all nonlinear systems are amenable to feedback linearization. Although the class of systems that are feedback linearizable is rich enough to make the theory important to control system designers, relatively few nontrivial aerospace applications (such as the ACMM) have been shown that use both state transformations and nonlinear feedback. Many aerospace applications appearing in the literature require no state transformation, which is in reality the most difficult part of the feedback linearization process to obtain. For example, if we consider the attitude control problem without momentum management, then no state transformation would be required and the feedback linearization can be obtained through nonlinear feedback alone. This is the spacecraft application of feedback linearization that appears most in the literature.

Coordinate Transformation to Normal Canonical Form

In this section, the nonlinear state transformation to normal form for the ACMM problem is discussed. The actual process for the solution of the set of partial differential equations will not be presented. Instead, only the coordinate transformation will be described.

Sheen and Bishop[16] have shown that the ACMM problem has relative degree $\{4, 3, 2\}$. This implies that the state transformation to normal canonical form will consist of a fourth-order, a third-order, and a second-order output function. Sheen and Bishop[16] selected as output functions $h_{B_3}^L$, $h_{B_2}^L$, and θ_3. In this paper, similar output functions have been chosen: $h_{B_3}^L$, $\eta h_{B_2}^L$, and $3\eta^3 I_{B_{12}}^L$. These output functions were chosen so that, in the fourth, third, and second derivatives, respectively, the coefficients on each control would be of the same form. This leads to a state transformation of the form $\boldsymbol{z} = \boldsymbol{\Phi}(\boldsymbol{x})$, where $\boldsymbol{z}^T = (\boldsymbol{z}_1^T, \boldsymbol{z}_2^T, \boldsymbol{z}_3^T)$, $\boldsymbol{x}^T = (\boldsymbol{\theta}^T, \boldsymbol{\omega}_B^{B^T}, \boldsymbol{h}_W^{B^T})$, and $\boldsymbol{\Phi}$ is a nonlinear function of $\boldsymbol{x}$. The nonlinear state transformation $\boldsymbol{z} = \boldsymbol{\Phi}(\boldsymbol{x})$ is given by

$$z_{1_1} = h_{B_3}^L \tag{18}$$

$$z_{1_2} = -\eta h_{B_1}^L \tag{19}$$

$$z_{1_3} = 3\eta^3 I_{B_{23}}^L - \eta^2 h_{B_3}^L \tag{20}$$

$$z_{1_4} = 3\eta^3\left\{\left(I_{B_{22}}^L - I_{B_{33}}^L\right)\omega_1^L - I_{B_{12}}^L\left(\omega_2^L + \eta\right) + I_{B_{13}}^L\omega_3^L\right\} + \eta^3 h_{B_1}^L \tag{21}$$

$$z_{2_1} = \eta h_{B_2}^L \tag{22}$$

$$z_{2_2} = 3\eta^3 I_{B_{13}}^L \tag{23}$$

$$z_{2_3} = 3\eta^3\left\{I_{B_{12}}^L\omega_1^L + \left(I_{B_{33}}^L - I_{B_{11}}^L\right)\left(\omega_2^L + \eta\right) - I_{B_{23}}^L\omega_3^L\right\} \tag{24}$$

$$z_{3_1} = 3\eta^3 I_{B_{12}}^L \tag{25}$$

$$z_{3_2} = 3\eta^3\left\{-I_{B_{13}}^L\omega_1^L + I_{B_{23}}^L\left(\omega_2^L + \eta\right) + \left(I_{B_{11}}^L - I_{B_{22}}^L\right)\omega_3^L\right\} \tag{26}$$

Taking time derivatives of z_{1_4}, z_{2_3}, or z_{3_2} will result in the appearance of the control. Because of the way that the output functions were selected, the derivatives in which the controls appear can be written in the form

$$\dot{\boldsymbol{z}}^* = \boldsymbol{b}(\boldsymbol{x}) + \boldsymbol{A}(\boldsymbol{x})\boldsymbol{u}^L \tag{27}$$

where $\boldsymbol{z}^* = (z_{1_4}, z_{2_3}, z_{3_2})^T$,

$$\boldsymbol{A}(\boldsymbol{x}) = -3\eta^3\boldsymbol{S}_1^L\left(\boldsymbol{I}_B^L\right)^{-1} \tag{28}$$

$$\begin{aligned}\boldsymbol{b}(\boldsymbol{x}) = \boldsymbol{a} + 3\eta^3\Big\{&\boldsymbol{S}_1^L\left(\boldsymbol{\eta} \times \boldsymbol{\omega}_B^L\right) + \boldsymbol{S}_2^L\left(\boldsymbol{\omega}_B^L + \boldsymbol{\eta}\right) \\ &- \left(\boldsymbol{\omega}_B^L + \boldsymbol{\eta}\right) \times \boldsymbol{S}_1^L\left(\boldsymbol{\omega}_B^L + \boldsymbol{\eta}\right) \\ &+ \boldsymbol{S}_1^L\left(\boldsymbol{I}_B^L\right)^{-1}\left(-\boldsymbol{\omega}_B^L \times \boldsymbol{I}_B^L\boldsymbol{\omega}_B^L + 3\eta^2\boldsymbol{k}_L^L \times \boldsymbol{I}_B^L\boldsymbol{k}_L^L\right)\Big\}\end{aligned} \tag{29}$$

$$\boldsymbol{S}_1^L = \begin{bmatrix} I_{B_{22}}^L - I_{B_{33}}^L & -I_{B_{12}}^L & I_{B_{13}}^L \\ I_{B_{12}}^L & I_{B_{33}}^L - I_{B_{11}}^L & -I_{B_{23}}^L \\ -I_{B_{13}}^L & I_{B_{23}}^L & I_{B_{11}}^L - I_{B_{22}}^L \end{bmatrix} \tag{30}$$

$$\boldsymbol{S}_2^L = \begin{bmatrix} \dot{I}_{B_{22}}^L - \dot{I}_{B_{33}}^L & 0 & 0 \\ 0 & \dot{I}_{B_{33}}^L - \dot{I}_{B_{11}}^L & 0 \\ 0 & 0 & \dot{I}_{B_{11}}^L - \dot{I}_{B_{22}}^L \end{bmatrix} \tag{31}$$

and $\boldsymbol{a} = (-\eta^2 z_{1_3}, 0, 0)^T$.

Linearizing Feedback

Given that the nonlinear dynamic system associated with the ACMM problem has been transformed to normal canonical form, a linearizing control feedback can be developed. The feedback control law is designed so that all of the nonlinear dynamics are canceled and the linear feedback can be used to place the closed-loop poles of the transformed states.

With a judicious choice of the control law, the transformed states z will behave linearly. If the desired trajectory for the states is given by z_d, then by choosing

$$\dot{z}^* = \boldsymbol{v} = \boldsymbol{K}(z_d - z) + \dot{z}_d^* \tag{32}$$

where $\dot{z}_d^*$ is the desired value of $\dot{z}^*$, the output functions will follow the desired trajectory with zero steady-state error (assuming that the desired signal is stable). With the gain matrix $\boldsymbol{K}$ given by

$$\boldsymbol{K} = \begin{bmatrix} k_{1_1} & k_{1_2} & k_{1_3} & k_{1_4} & 0 & 0 & 0 & 0 & 0 \\ 0 & 0 & 0 & 0 & k_{2_1} & k_{2_2} & k_{2_3} & 0 & 0 \\ 0 & 0 & 0 & 0 & 0 & 0 & 0 & k_{3_1} & k_{3_2} \end{bmatrix} \tag{33}$$

the equivalent linear system has the characteristic equation

$$\lambda = \left(s^4 + k_{1_4}s^3 + k_{1_3}s^2 + k_{1_2}s + k_{1_1}\right) \times \left(s^3 + k_{2_3}s^2 + k_{2_2}s + k_{2_1}\right)\left(s^2 + k_{3_2}s + k_{3_1}\right) \tag{34}$$

We must select $\boldsymbol{K}$ so that the characteristic equation has the desired roots. This leads to the nonlinear control law $\boldsymbol{u}^L = [\boldsymbol{A}(\boldsymbol{x})]^{-1}[-\boldsymbol{b}(\boldsymbol{x}) + \boldsymbol{v}]$, which after expanding yields

$$\begin{aligned} \boldsymbol{u}^L = {} & \boldsymbol{I}_B^L\left(\boldsymbol{\eta} \times \boldsymbol{\omega}_B^L\right) - \boldsymbol{\omega}_B^L \times \boldsymbol{I}_B^L\boldsymbol{\omega}_B^L + 3\eta^2\boldsymbol{k}_L^L \times \boldsymbol{I}_B^L\boldsymbol{k}_L^L \\ & - \boldsymbol{I}_B^L\left(\boldsymbol{S}_1^L\right)^{-1}\left\{\left(\boldsymbol{\omega}_B^L + \boldsymbol{\eta}\right) \times \boldsymbol{S}_1^L\left(\boldsymbol{\omega}_B^L + \boldsymbol{\eta}\right) - \boldsymbol{S}_2^L\left(\boldsymbol{\omega}_B^L + \boldsymbol{\eta}\right)\right\} \\ & - (1/3\eta^3)\boldsymbol{I}_B^L\left(\boldsymbol{S}_1^L\right)^{-1}\left\{\dot{z}_d^* - \boldsymbol{a} + \boldsymbol{K}(z_d - z)\right\} \end{aligned} \tag{35}$$

Ultimately we want the control torque $\boldsymbol{u}$ in the B frame. Therefore, $\boldsymbol{u}^L$ is transformed to the B frame via

$$\boldsymbol{u}^B = \boldsymbol{T}^{BL}\boldsymbol{u}^L \tag{36}$$

Eqs. (35) and (36) represent the nonlinear control law to be used by the spacecraft for ACMM.

Two important issues must still be addressed before the given nonlinear control law can be used. First, the invertibility of the state transformation must be examined to determine if and when the control law is valid. Second, the selection of the gains k_{i_j}, given in $\boldsymbol{K}$, must be discussed to determine desirable closed-loop pole locations.

Control Law Singularities

The nonlinear transformation $z = \boldsymbol{\Phi}(\boldsymbol{x})$ is not a global transformation and is only valid in a region around a particular equilibrium point. The regions where the nonlinear control law is valid are represented by all of the points where the matrix $\boldsymbol{A}(\boldsymbol{x})$ is nonsingular. Because $\boldsymbol{A}(\boldsymbol{x}) = -3\eta^3\boldsymbol{S}_1^L(\boldsymbol{I}_B^L)^{-1}$, its inverse is given by

$$[\boldsymbol{A}(\boldsymbol{x})]^{-1} = -(1/3\eta^3)\boldsymbol{I}_B^L\left(\boldsymbol{S}_1^L\right)^{-1} \tag{37}$$

Therefore, the invertibility of $\boldsymbol{A}(\boldsymbol{x})$ is dependent on the invertibility of $\boldsymbol{S}_1^L$. For $\boldsymbol{S}_1^L$ to be invertible, Δ must be nonzero, where Δ is the determinant of $\boldsymbol{S}_1^L$ and is determined to be

$$\begin{aligned} \Delta = {} & \left(I_{B_{11}}^L - I_{B_{22}}^L\right)\left(I_{B_{22}}^L - I_{B_{33}}^L\right)\left(I_{B_{33}}^L - I_{B_{11}}^L\right) \\ & + \left(I_{B_{11}}^L - I_{B_{22}}^L\right)\left(I_{B_{12}}^L\right)^2 + \left(I_{B_{33}}^L - I_{B_{11}}^L\right)\left(I_{B_{13}}^L\right)^2 \\ & + \left(I_{B_{22}}^L - I_{B_{33}}^L\right)\left(I_{B_{23}}^L\right)^2 \end{aligned} \tag{38}$$

If the inertia matrix is written in the L frame as $\boldsymbol{I}_B^L = \boldsymbol{T}^{LP}\boldsymbol{I}_B^P\boldsymbol{T}^{PL}$, then Δ can be expressed as

$$\Delta = \left(I_{B_1}^P - I_{B_2}^P\right)\left(I_{B_2}^P - I_{B_3}^P\right)\left(I_{B_3}^P - I_{B_1}^P\right)\Lambda\left(\theta_r^*, \theta_p^*, \theta_y^*\right) \tag{39}$$

where Λ is a function of the principal Euler angles relating the L frame to the P frame. For a pitch–yaw–roll principal Euler rotation sequence, $\Lambda(\theta_r^*, \theta_p^*, \theta_y^*)$ can be written as

$$\begin{aligned} \Lambda\left(\theta_r^*, \theta_p^*, \theta_y^*\right) = {} & \cos 2\theta_r^* \cos 2\theta_p^* \cos 2\theta_y^* \\ & + \sin 2\theta_r^* \sin 2\theta_p^* \sin\theta_y^*\left(\tfrac{1}{4} - \tfrac{3}{4}\cos 2\theta_y^*\right) \end{aligned} \tag{40}$$

For Δ to be nonzero, the following conditions must be true: $I_{B_1}^P \neq I_{B_2}^P$, $I_{B_2}^P \neq I_{B_3}^P$, $I_{B_3}^P \neq I_{B_1}^P$, and $\Lambda \neq 0$. The first three conditions are physical attributes of the spacecraft being analyzed and, as such, limit which spacecraft are candidates for use of the nonlinear control law. The final condition, that Λ be nonzero, imposes certain constraints on the Euler angle orientations that the spacecraft can achieve. The inertia constraints, $I_{B_1}^P \neq I_{B_2}^P$, $I_{B_2}^P \neq I_{B_3}^P$, and $I_{B_3}^P \neq I_{B_1}^P$, are inherent to the ACMM problem and even appear in the design of linear controllers.[11] Therefore, any ACMM design can only be used on spacecraft where none of the principal inertias are equal.

At any TEA the value of Λ will be either -1 (a local minimum) or 1 (a local maximum), which implies that the TEAs are not singular points of the control law and that all of the TEAs are located as far as they can be from the singularity.[24] Therefore, operation of the nonlinear control law around the TEA should avoid all of the singular points. However, initial orientations near the TEA do not guarantee that the state trajectories will not induce the singularity. If, for instance, an initial angular rate is large, it is possible that the controller will be unable to slow the spacecraft angular rate before a singular attitude orientation is reached. Therefore, the ability of the nonlinear controller to drive the spacecraft to a TEA and avoid the singularity is dependent on the initial conditions.

TEA in Transformed States

Recall Eq. (14) for the total angular momentum of the spacecraft system, but written in the LVLH frame. At TEA, $I_{B_{12}}^L = I_{B_{13}}^L = I_{B_{23}}^L = 0$, $\boldsymbol{\omega}_B^L = -\boldsymbol{\eta}$, and $h_{W_1}^L = h_{W_3}^L = 0$. Therefore, the total angular momentum at a TEA must be

$$\boldsymbol{h}_B^L = \begin{pmatrix} 0 \\ h_{W_2}^L \\ 0 \end{pmatrix} + \begin{bmatrix} I_{B_i}^P & 0 & 0 \\ 0 & I_{B_j}^P & 0 \\ 0 & 0 & I_{B_k}^P \end{bmatrix}\begin{pmatrix} 0 \\ -\eta \\ 0 \end{pmatrix} = \begin{pmatrix} 0 \\ h_{W_2}^L - I_{B_j}^P\eta \\ 0 \end{pmatrix} \tag{41}$$

where $i \neq j$, $j \neq k$, $k \neq i$, and the $I_{B_i}^P$ represent the principal inertias. Because the ultimate goal of investigating a TEA in the transformed states is to develop a desired operating point for the system, and because a TEA can exist with an arbitrary value of $h_{W_2}^L$, the value of $h_{W_2}^L$ is chosen to be zero at TEA. Also, the desired orientation of the spacecraft is such that Y_L is aligned with Y_P. Therefore, the desired value for z should be $z_d = (0, 0, 0, 0, -I_{B_2}^P\eta^2, 0, 0, 0, 0)^T$.

Adaptive Controller Design

In the preceding sections, a nonlinear control law was developed based on known spacecraft mass properties. In reality, the actual mass properties may not be known precisely. For spacecraft with a limited number of moving appendages, determining the inertia of the spacecraft might be practical using onboard sensors to measure

the locations and orientations of individual components for mass property calculations. However, for large spacecraft, with possibly many moving appendages and varying configurations, such an inertia computation system can become expensive (both monetarily and computationally) and physically burdensome, because of numerous sensors and connections. Another option is to book keep using the scheduled movements of the onboard pieces, but this requires previous knowledge of the locations of each portion of the spacecraft. Therefore, for spacecraft whose mass properties cannot be directly sensed, a different approach must be developed. We investigate here an indirect method for determining the spacecraft inertia, so that the attitude control and momentum manager can adapt to changes in spacecraft configurations.

Indirect Adaptive Control

Adaptive controllers, as their name implies, can learn about their surroundings and modify themselves to account for changes in the dynamic system being controlled. In this learning environment, the adaptive controller can change internal parameters, so that certain closed-loop design parameters can be maintained, such as natural frequency, damping ratio, settling time, etc. It is this tailoring of the control law that can allow an adaptive controller to stabilize time-varying systems, which might otherwise lead to instability in systems utilizing fixed-parameter controllers.

There are two basic types of adaptive controllers: direct and indirect. Direct adaptive controllers explicitly change their controller parameters based on the closed-loop performance of the entire system. Indirect adaptive controllers, on the other hand, determine system parameters from the closed-loop dynamics and then use the updated system information to redesign the control law.

Indirect adaptive controllers are essentially composed of an inner and an outer loop.[21] The time-varying system and basic control law form the inner loop. The outer loop consists of a parameter estimator, which performs recursive estimation of system parameters, and a controller redesign, which adjusts the parameters in the basic control law based on the new system parameter estimates and any design constraints.

Selection of a direct or indirect adaptive controller is dependent on the system or process being controlled and the complexity of the dynamic models being used for design. The dynamic models associated with the ACMM design problem are functions of the Euler angles, the body angular rates, the total CMG momentum, the interactive control torque, the orbital rate, and the inertia matrix of the entire spacecraft. Of these, only the elements of the inertia matrix are considered changing system parameters (the orbital rate is assumed to be maintained at a constant value through other means). The nonlinear control law is a function of the same variables as the dynamic models, plus the gain matrix $\boldsymbol{K}$ and the desired state trajectories defined by $\boldsymbol{z}_d$. The gain matrix $\boldsymbol{K}$ is dependent only on the design specifications, inasmuch as $\boldsymbol{K}$ defines the locations of the closed-loop poles of the transformed system. If, for now, the desired state trajectories are assumed to be externally supplied, then the only changing parameters in the control law will be the elements of the inertia matrix. Therefore, an adaptive scheme that can determine the spacecraft mass properties is needed. An indirect adaptive controller is investigated here.

Because the gain matrix $\boldsymbol{K}$ in Eq. (35) is predetermined based on the design specifications, there is no need to perform a controller redesign in the adaptive scheme given for a self-tuning regulator. Instead, the estimated inertia matrix can be used directly by the controller to stabilize the system during mass property changes. Because the spacecraft dynamics and the nonlinear control law have already been established, all that remains in the construction of the adaptive ACMM system is the mass property estimator.

Mass Property Estimation

According to Åström and Wittenmark,[21] "on-line determination of process parameters is a key element in adaptive control." This implies that a good model of the dynamics is needed: one that, with the proper parameters, adequately describes the motion. The determination of process parameters requires estimation algorithms capable of real-time evaluation. For the spacecraft adaptive ACMM control scheme, the parameters that need to be determined are the mass properties corresponding to the dynamical model, i.e., the full inertia matrix. The continuous-discrete EKF is a well-demonstrated method of performing estimation for nonlinear systems. Because of the (generally) good results obtained with the EKF, and because of its history of use on-orbit for a variety of purposes, the EKF is selected here as the mass property estimator.

When the EKF is supplied with measurements of $\boldsymbol{\theta}$, $\boldsymbol{\omega}_B^B$, and $\boldsymbol{h}_W^B$, it can serve a dual purpose. Not only can it give estimates of the mass properties, but it can also provide filtered values of the dynamic states for the nonlinear control law or other onboard users.

The dynamic states that will be required by the controller are $\boldsymbol{\theta}$, $\boldsymbol{\omega}_B^B$, and $\boldsymbol{h}_W^B$. To provide an estimate of these states, as well as the elements of the inertia matrix, an augmented state vector is defined as $\boldsymbol{x}_\star^T = (\boldsymbol{x}^T, \boldsymbol{p}^T)$, where $\boldsymbol{p}^T = (I_{B_{11}}^B, I_{B_{22}}^B, I_{B_{33}}^B, I_{B_{12}}^B, I_{B_{13}}^B, I_{B_{23}}^B)$. The inertia elements are slowly time varying and are modeled via $\dot{\boldsymbol{p}} = \boldsymbol{\zeta}_p$, where $\boldsymbol{\zeta}_p$ is a white Gaussian noise process. Then the augmented system dynamics can be given by

$$\dot{\boldsymbol{x}}_\star = \boldsymbol{f}(\boldsymbol{x}_\star, \boldsymbol{u}) + \boldsymbol{\zeta} \tag{42}$$

where

$$\boldsymbol{f}(\boldsymbol{x}_\star, \boldsymbol{u}) = \begin{pmatrix} \boldsymbol{R}\boldsymbol{\omega}_B^B + \boldsymbol{\eta} \\ \left(\boldsymbol{I}_B^B\right)^{-1}\left(-\boldsymbol{\omega}_B^B \times \boldsymbol{I}_B^B\boldsymbol{\omega}_B^B + 3\eta^2\boldsymbol{k}_L^B \times \boldsymbol{I}_B^B\boldsymbol{k}_L^B - \boldsymbol{u}^B\right) \\ -\boldsymbol{\omega}_B^B \times \boldsymbol{h}_W^B + \boldsymbol{u}^B \\ \boldsymbol{O}_{6\times 1} \end{pmatrix} \tag{43}$$

where $\boldsymbol{\zeta}$ is a white Gaussian noise process associated with the entire augmented system and $\boldsymbol{O}_{6\times 1}$ is a six by one array of zeros. The noise in the dynamic states is due to unmodeled dynamics and modeling errors. The noise characteristics of $\boldsymbol{\zeta}$ are given by $E[\boldsymbol{\zeta}(t)\boldsymbol{\zeta}^T(\tau)] = \boldsymbol{Q}\delta(t-\tau)$, where $\boldsymbol{Q}$ is the spectral density matrix of $\boldsymbol{\zeta}$ and δ is the Dirac delta function.

Measurements of the Euler angles, body angular rates, and the total CMG momentum are assumed to be available for measurement by the controller. Each of these measurements is assumed to be corrupted by white Gaussian noise and available at times $\{t_k\}$, so that the measurement model is

$$\boldsymbol{y}_k = \boldsymbol{C}\boldsymbol{x}_\star(t_k) + \boldsymbol{\nu}_k \tag{44}$$

where $\boldsymbol{C} = [\boldsymbol{I}_{9\times 9} \;\; \boldsymbol{O}_{9\times 6}]$, $\{\boldsymbol{\nu}_k\}$ is a sequence of measurement noise vectors with $E[\boldsymbol{\nu}_j\boldsymbol{\nu}_k^T] = \boldsymbol{R}\delta_{jk}$, $\boldsymbol{I}_{9\times 9}$ is a nine by nine identity matrix, and $\boldsymbol{O}_{9\times 6}$ is a nine by six matrix of zeros; $\boldsymbol{R}$ is the measurement covariance matrix.

Mass Property Observability and Probing Signals

The ability of any parameter identification scheme to estimate system parameters is dependent on the system's observability. The observability of a system indicates whether or not each state in that system can be uniquely determined from a given set of measurements. If any of the states cannot be uniquely determined, then those states are said to be unobservable. Therefore, for the mass properties of a spacecraft to be properly estimated, each of the elements of the inertia matrix must be observable based on measurements of $\boldsymbol{\theta}$, $\boldsymbol{\omega}_B^B$, and $\boldsymbol{h}_W^B$.

Previous investigations have shown that mass property estimation is not possible at the TEA, where the complete inertia matrix is unobservable.[11,18] We know that the attitude control and momentum manager drives the spacecraft to the TEA. Therefore, there is a fundamental conflict between ACMM and mass property estimation. In an effort to enhance observability, a small amplitude probing signal is used to induce attitude motion about the TEA. The selection of a probing signal that can generate sufficient motion, so that the EKF properly estimates the mass properties of the spacecraft, is crucial to the effectiveness of the adaptive nonlinear controller. At the same time, the motion should not be so large that proper spacecraft attitude cannot be maintained. Some compromise must be made between good estimation and small attitude excursions.

Previous investigations[11,18] have shown that sinusoidal probing signals can generate adequate attitude motion for accurate mass

property estimation. Although there are probably probing signals that offer greater observability in some optimal sense, for simplicity, the probing signals are chosen here to be sinusoidal.

To avoid exciting the bending modes of the spacecraft, the probing signal frequency must be chosen well below the lower bound of the structural modes. Therefore, both the amplitude and the frequency of the probing signals must be addressed, so that a desirable response can be achieved without violating other system constraints.

Unfortunately, if the nonlinear transformation and nonlinear control law are used, a desired trajectory z_d can be difficult to develop. Performing the nonlinear transformation on the desired attitude deviations can lead to complicated functions in the z coordinates. Therefore, to avoid performing this nonlinear transformation, another method of selecting z_d must be developed.

Suppose that the desired small attitude deviations for a spacecraft about the TEA are given by

$$\theta^*_{i_d} = \alpha_i \sin \kappa_i t \qquad \text{for} \qquad i = r, p, y \tag{45}$$

where α_i and κ_i are, respectively, the amplitude and the frequency of the deviation in the principal Euler angles. To generate $\boldsymbol{\theta}^*_d$, a new desired trajectory in the z coordinates must be developed. Because the desired small attitude deviations occur around the TEA, the behavior of the nonlinear output functions ($h^L_{B_3}$, $\eta h^L_{B_3}$, and $3\eta^3 I^L_{B_{12}}$) near the TEA can be used to linearize the transformation and develop a desired z_d.

A desired trajectory for z, which produces (approximately) the desired attitude deviations around the TEA, is given by

$$z_{1_{1_d}} = \frac{3\eta^2\alpha_1\left(I^P_{B_2} - I^P_{B_3}\right)}{\kappa_1^2 - \eta^2}(\kappa_1 \sin \eta t - \eta \sin \kappa_1 t) \tag{46}$$

$$z_{2_{1_d}} = -I^P_{B_2}\eta^2 - 3\eta^3\alpha_2\left(I^P_{B_3} - I^P_{B_1}\right)\cos \kappa_2 t \tag{47}$$

$$z_{3_{1_d}} = 3\eta^3\alpha_3\left(I^P_{B_1} - I^P_{B_2}\right)\sin \kappa_3 t \tag{48}$$

The remaining elements of z_d and $\dot{z}^*_d$ are generated by taking the appropriate time derivatives of the output functions. These signals were obtained by linearizing the expressions for $I^L_{B_{12}}$, $I^L_{B_{13}}$, and $I^L_{B_{23}}$ [given in Eq. (11)] about the TEA at $\boldsymbol{\theta}^* = (0, 0, 0)^T$ and using them in Eqs. (20), (23), and (25) (Ref. 25).

In the adaptive scenario, the values of the $I^P_{B_i}$ are not precisely known. However, approximate values for the principal inertias can be obtained by computing the eigenvalues of $\hat{\boldsymbol{I}}^B_B$, the estimated inertia matrix. Therefore, an approximate desired probing signal can be generated.

Adaptive ACMM

Figure 1 shows the complete adaptive control scheme for attitude control and momentum management. It shows the three basic components of the adaptive controller: the EKF, the probing signal generator, and the nonlinear controller. The EKF uses measurements of the spacecraft dynamic states and the current interactive control torque to generate the current state estimates, as well as mass property estimates. The estimates of the spacecraft inertia matrix are then provided to the probing signal generator and the nonlinear control law. The probing signal generator combines the desired attitude deviations with the current inertia estimates to produce the desired input signal for the feedback linearized controller. Then the nonlinear controller uses the current estimates of the mass properties, the current estimates of the dynamic states, and the desired input signal to generate the interactive control torque $\boldsymbol{u}^B$.

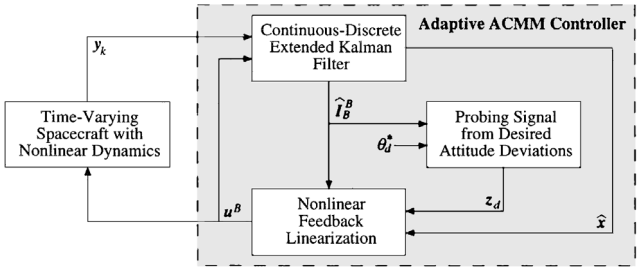

Fig. 1 Complete adaptive ACMM controller.

Simulation Results

To verify that the adaptive nonlinear controller properly stabilizes the closed-loop system, numerous simulations were performed. In the case presented here, the spacecraft considered is the International Space Station (ISS) after flight 4O-12R and in orbit around the Earth. The large inertia changes are generated by simulating the motion of a large mass attached to the spacecraft.

Simulation Environment

Simulation of the spacecraft attitude dynamics was performed in a realistic environment, which included the effects of nonrigid body dynamics (but not flexible structural dynamics), atmospheric drag, and higher-order gravity terms. The system of equations contained in the simulation environment included the orbital dynamics, the attitude dynamics, and the CMG dynamics, including Kennel's CMG steering law. The dynamics associated with three rotating solar panels, one large translating mass, and seven onboard CMGs were included in these equations of motion. The CMGs can store 32,000 ft-lb of angular momentum. The atmosphere was modeled using the 1970 Jacchia density model, and the aerodynamic drag was computed based on the projected cross-sectional area of the spacecraft in the direction of the relative wind of a rotating atmosphere. The higher-order gravity terms, J_2–J_4, were also included in the simulation environment.

The ISS Alpha has a nominal inertia matrix defined by $I^B_{11} = 70.9899 \times 10^6$, $I^B_{22} = 55.6448 \times 10^6$, $I^B_{33} = 114.5910 \times 10^6$, $I^B_{12} = -1.9567 \times 10^6$, $I^B_{13} = -5.2120 \times 10^6$, and $I^B_{23} = 0.0509 \times 10^6$ slug-ft^2, and its principal inertias are $I_1 = 7.0626 \times 10^7$, $I_2 = 5.5393 \times 10^7$, and $I_3 = 1.1521 \times 10^8$ slug-ft^2. To simulate a moving payload onboard the ISS, a 500-slug mass, with an inertia matrix defined by $I_{11} = I_{22} = I_{33} = 10{,}000$ slug-ft^2, and $I_{12} = I_{13} = I_{23} = 0$, traverses the spacecraft. The mass starts at the center of mass of the nominal ISS at $t = 0$. During the first 20,000 s, the mass is stationary. From 20,000 to 40,000 s, the mass moves 100 ft in the x direction. Next, the mass moves 100 ft in the y direction from 40,000 to 60,000 s. The mass then moves an additional 100 ft in the z direction from 60,000 to 100,000 s, where it remains for the duration of the simulation. These particular motions are used only to demonstrate the adaptiveness of the controller to changes in the TEA and do not represent any known operational mode.

For this simulation, the initial conditions were selected so that the CMGs do not saturate during the initial transient and are given by $\boldsymbol{\theta}_0 = (-1, 7, 7)^T$ deg, $\boldsymbol{\omega}^B_{B_0} = -\boldsymbol{\eta}$, and $\boldsymbol{h}^B_0 = (0, 0, 0)^T$ ft-lb-s. The orbital rate η is 0.0011 rad/s, so that one orbit takes 5712 s and the orbital inclination is 50 deg. The measurements of $\boldsymbol{\theta}$, $\boldsymbol{\omega}^B_B$, and $\boldsymbol{h}^B_W$ are assumed to be available every 30 s. Also, the measurements are corrupted by noise. For this case the standard deviations for the measurement noises are 2×10^{-3} rad for Euler angles, 1×10^{-5} rad/s for angular rates, and 100 ft-lb-s for CMG momentum.

In previous investigations,[1,2,11,16] the real portions of the closed-loop poles have been selected near $-\eta$. This region in the complex plane offers relatively fast response, while avoiding excitation of the spacecraft's structural modes. Therefore, the closed-loop poles will be placed so that their real parts are between $-\eta/2$ and $-\eta$. In particular, the nine poles will be selected so that they are equally distributed along the circle of radius η between $-\eta/2$ and $-\eta$. These closed-loop pole locations correspond to the following points in the complex plane: $-\eta$, $-\eta e^{\pm\pi i/12}$, $-\eta e^{\pm\pi i/6}$, $-\eta e^{\pm\pi i/4}$, and $-\eta e^{\pm\pi i/3}$. This distribution of poles provides the desired performance characteristics.

Keep in mind that the closed-loop poles mentioned in this section correspond to the linear response of the transformed states. The response of the original states can be expected to behave in a nonlinear way. This can potentially lead to undesirable response trajectories. Therefore, care must be exercised in the design, to avoid unwanted response characteristics.

The probing signal parameters correspond to principal Euler angle oscillations with an amplitude of 1.5 deg. The probing signals are

defined by

$$\theta^* = \begin{pmatrix} 1.5\sin 4\eta t \\ 1.5\sin[4\eta t - (\pi/6)] \\ 1.5\sin[3\eta t + (\pi/4)] \end{pmatrix} \text{deg} \tag{49}$$

The amplitudes and frequencies of the probing signals were chosen to provide adequate motion for mass property observability.[11,25]

Results

The attitude history of the spacecraft during the mass property changes is given in Fig. 2 and shows that the spacecraft makes small oscillations about the TEA. The oscillations are less than 2 deg in amplitude and the period of each oscillation is greater than 15 min. As the mass properties change, the attitude of the spacecraft changes to reach a new TEA. Initially, the expected TEA is at $\theta = (-0.6, 6.8, 7.3)$ deg, then due to the changes in the mass properties,

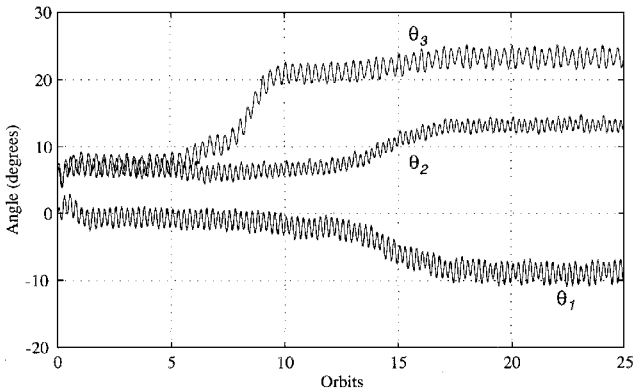

Fig. 2 Attitude history during translating mass simulation.

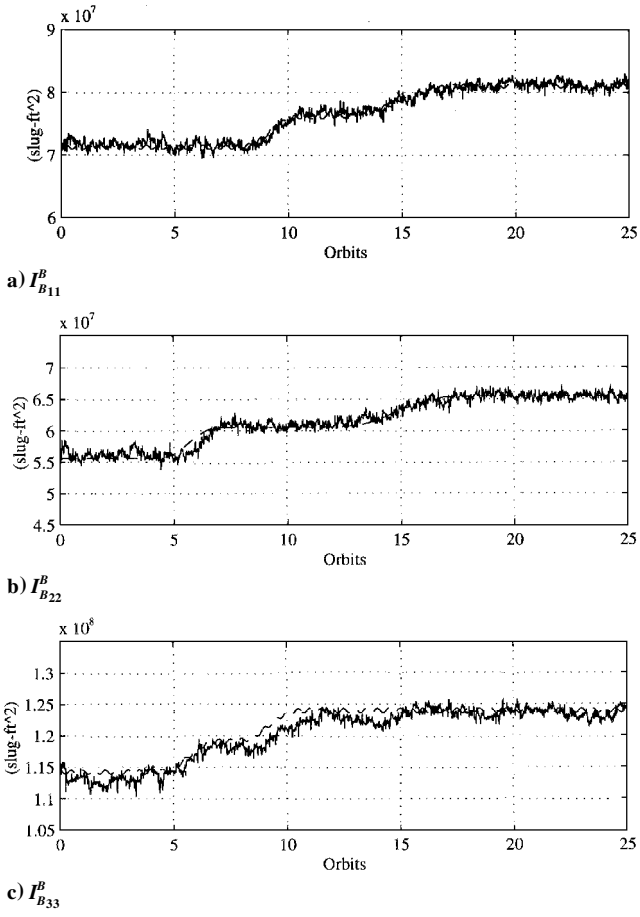

Fig. 3 Moments of inertia during translating mass simulation: ——, estimate and – – –, actual.

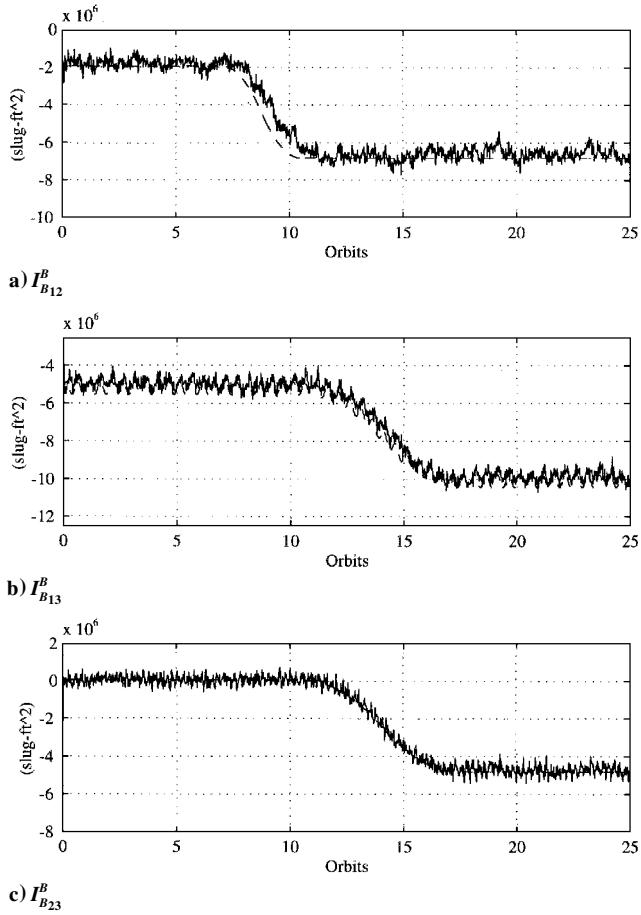

Fig. 4 Cross products of inertia during translating mass simulation: ——, estimate and – – –, actual.

after about 18 orbits, the expected TEA is at $\theta = (-8.4, 13.3, 22.8)$ deg.

During the entire simulation, the adaptive nonlinear controller estimates the mass properties and utilizes them to update the control law. Figures 3 and 4 show how the mass property estimator is performing. The true values are shown with dashed lines, whereas the estimates are shown with solid lines. The oscillations in the true values of $I^B_{B_{11}}$, $I^B_{B_{33}}$, and $I^B_{B_{13}}$ are caused by the rotating solar panels. The large ramp changes in the mass properties are generated by the changes in position of the translating mass. These plots indicate that the estimates of the moments of inertia are always within 6% (and generally within 2%) of the true values and that the estimator can track the changes in the inertias. The estimates tend to have about a 1- or 2-orbit lag in the estimates of the moments of inertia and in $I^B_{B_{12}}$. Small error biases exist in the estimates of $I^B_{B_{12}}$. The lags and biases in the estimates can be reduced or eliminated through the use of a larger amplitude probing signal. However, a larger signal may lead to CMG saturation.

The magnitude of the stored CMG momentum during the translating mass simulation is always less than the CMG momentum limit of 32,000 ft-lb-s, and the stored momentum is generally less than 15,000 ft-lb-s. Also, the required CMG torque never exceeds 90 ft-lb in magnitude.

Issues

The required control torques are cyclic in nature, which results in the continuous use of actuators that change the orientations of the control moment gyro's gimbals. This can potentially reduce the lifespan of the control moment gyros. Therefore, for practical purposes, the controller might only be adaptive (estimating the mass properties) during expected mass property changes, and during acquiescent periods, the most recent inertia estimates would be used by the nonlinear controller. This would reduce the attitude deviations and the control moment gyro workload.

A potential problem can arise from the use of the inertia matrix estimates. If the estimates of the inertias are such that two of the computed principal inertias are approximately equal to one another (even though the true values are not), the singularity in the control law may be induced, resulting in a large, unexpected control torque. Therefore, the singularity condition should be checked. This can easily be accommodated in the flight code.

The nonlinear control law was based on the assumption that the spacecraft is slowly time varying. If, in fact, the spacecraft violates this assumption, then it is possible that the unmodeled dynamics (which are not canceled by the nonlinear controller) can cause instability in the closed-loop system (even if the mass properties are known exactly). Therefore, it is important to determine exactly how fast the variations in the spacecraft can occur before the nonlinear controller can no longer stabilize the system, so that potentially destabilizing onboard maneuvers can be avoided.

In this paper, the mass property variations are slowly time-varying and the EKF converges as desired. However, larger or faster variations could possibly lead to poor filter response or even divergence. Therefore, the effect of mass property variations on the performance of the EKF needs to be fully assessed.

Because the probing signals were chosen without considering the efficiency of motion, they may not provide the best motion for sufficient estimation of the mass properties. It may be possible to find a more optimal probing signal: one that offers the most observability with the least motion.

Conclusions

The proposed adaptive nonlinear controller performs its desired function: it stabilizes the spacecraft while simultaneously performing CMG momentum management utilizing gravity gradient torques to unload momentum. Real-time estimates of the mass properties during inertia changes are a by-product of the controller process, as well as filtered values of spacecraft Euler angles, body rates, and CMG momentum. The proposed controller solves the ACMM problem in a very implementable fashion. The modular structure allows implementation of the nonlinear controller without mass property identification, the mass property identification without the nonlinear controller, or both together.

Acknowledgments

The authors would like to acknowledge the guidance of John W. Sunkel from NASA Johnson Space Center during the course of this work. Also, Carlos Roithmayr of NASA Johnson Space Center is gratefully acknowledged for his verification of the multibody dynamical equations of motion, which were used in the simulation environment.

References

[1]Wie, B., Byun, K. W., Warren, V. W., Geller, D., Long, D., and Sunkel, J., "New Approach to Attitude/Momentum Control for the Space Station," *Journal of Guidance, Control, and Dynamics*, Vol. 12, No. 5, 1989, pp. 714–722.

[2]Sunkel, J. W., and Shieh, L. S., "An Optimal Momentum Management Controller for the Space Station," *Journal of Guidance, Control, and Dynamics*, Vol. 13, No. 4, 1990, pp. 659–668.

[3]Wie, B., Hu, A., and Singh, R., "Multi-Body Interaction Effects on Space Station Attitude Control and Momentum Management," *Journal of Guidance, Control, and Dynamics*, Vol. 13, No. 6, 1990, pp. 993–999.

[4]Byun, K. W., Wie, B., Geller, D., and Sunkel, J., "Robust H_∞ Control Design for the Space Station with Structured Parameter Uncertainty," *Journal of Guidance, Control, and Dynamics*, Vol. 14, No. 6, 1991, pp. 1115–1122.

[5]Elgersma, E., Stein, G., Jackson, M., and Yeichner, J., "Robust Controllers for Space Station Momentum Management," *IEEE Control Systems Magazine*, Vol. 12, No. 2, 1992, pp. 14–22.

[6]Balas, G. J., Packard, A. K., and Harduvel, J. T., "Application of μ-Synthesis Technique to Momentum Management and Attitude Control of the Space Station," *Proceedings of AIAA Guidance, Navigation, and Control Conference* (New Orleans, LA), AIAA, Washington, DC, 1991, pp. 565–575.

[7]Rhee, I., and Speyer, J. L., "Robust Momentum Management and Attitude Control System for the Space Station," *Journal of Guidance, Control, and Dynamics*, Vol. 15, No. 2, 1992, pp. 342–351.

[8]Burns, T. F., and Flashner, H., "Adaptive Control Applied to Momentum Unloading Using the Low Earth Orbital Environment," *Journal of Guidance, Control, and Dynamics*, Vol. 15, No. 2, 1992, pp. 325–333.

[9]Zhao, X. M., Shieh, L. S., Sunkel, J. W., and Yuan, Z. Z., "Self-Tuning Control of Attitude and Momentum Management for the Space Station," *Journal of Guidance, Control, and Dynamics*, Vol. 15, No. 1, 1992, pp. 17–27.

[10]Parlos, A. G., and Sunkel, J. W., "Adaptive Attitude Control and Momentum Management for Large-Angle Spacecraft Maneuvers," *Journal of Guidance, Control, and Dynamics*, Vol. 15, No. 4, 1992, pp. 1018–1028.

[11]Paynter, S. J., "Adaptive Control of the Space Station," M.S. Thesis, Dept. of Aerospace Engineering and Engineering Mechanics, Univ. of Texas, Austin, TX, Dec. 1992.

[12]Vadali, S. R., and Oh, H.-S., "Space Station Attitude Control and Momentum Management: A Nonlinear Look," *Journal of Guidance, Control, and Dynamics*, Vol. 15, No. 3, 1992, pp. 577–586.

[13]Singh, S. N., and Bossart, T. C., "Feedback Linearization and Nonlinear Ultimate Boundedness Control of the Space Station Using CMG," *Proceedings of the AIAA Guidance Navigation and Controls Conference*, Vol. 1, AIAA, Washington, DC, 1990, pp. 369–376 (AIAA Paper 90-3354).

[14]Singh, S. N., and Bossart, T. C., "Invertibility of Map, Zero Dynamics and Nonlinear Control of Space Station," *Proceedings of the AIAA Guidance, Navigation, and Controls Conference*, Vol. 1, AIAA, Washington, DC, 1991, pp. 576–584 (AIAA Paper 91-2663).

[15]Singh, S. N., and Iyer, A., "Nonlinear Regulation of Space Station: A Geometric Approach," *Journal of Guidance, Control, and Dynamics*, Vol. 17, No. 2, 1994, pp. 242–249.

[16]Sheen, J. J., and Bishop, R. H., "Spacecraft Nonlinear Control," *Journal of Astronautical Sciences*, Vol. 42, No. 3, 1994, pp. 361–377.

[17]Dzielski, J., Bergmann, E., Paradiso, J., Rowell, D., and Wormley, D., "Approach to Control Moment Gyroscope Steering Using Feedback Linearization," *Journal of Guidance, Control, and Dynamics*, Vol. 14, No. 1, 1991, pp. 96–106.

[18]Sheen, J. J., and Bishop, R. H., "Adaptive Nonlinear Control of Spacecraft," *Journal of Astronautical Sciences*, Vol. 42, No. 4, 1994, pp. 451–472.

[19]Paynter, S. J., "Adaptive Nonlinear Attitude Control of the Space Station," AIAA Paper 94-0014, Jan. 1994.

[20]Dzielski, J. E., "A Feedback Linearization Approach to Spacecraft Control Using Momentum Exchange Devices," Ph.D. Thesis, Dept. of Aeronautics and Astronautics, Massachusetts Inst. of Technology, Cambridge, MA, April 1988.

[21]Åström, K. J., and Wittenmark, B., *Adaptive Control*, Addison–Wesley, Reading, MA, 1989, p. 58 and Chaps. 3 and 5.

[22]Isidori, A., *Nonlinear Control Systems*, 2nd ed., Springer–Verlag, Berlin, 1989, Chaps. 4 and 5.

[23]Slotine, J. E., and Li, W., *Applied Nonlinear Control*, Prentice–Hall, Englewood Cliffs, NJ, 1991, Chap. 6.

[24]Paynter, S. J., and Bishop, R. H., "The Singularities of Nonlinear Attitude Control and Momentum Management," AIAA Paper 97-0111, Jan. 1997.

[25]Paynter, S. J., *Indirect Adaptive Nonlinear Attitude Control and Momentum Management of Spacecraft*, Ph.D. Dissertation, Dept. of Aerospace Engineering and Engineering Mechanics, Univ. of Texas, Austin, TX, Dec. 1995.